



**NIST Interagency Report
NIST IR 8436**

**Bounding the Structure Separation
Distance**

*A Modeling Study in Support of the Structure Separation
Experiments Project*

Kuldeep Prasad
Alexander Maranghides
Eric Link
Shonali Nazare
Matthew Hoehler
Matthew Bundy
Rodney Bryant
Steve Hawks
Frank Bigelow
William (Ruddy) Mell
Anthony Bova
Tom Milac
Daniel Gorham
Faraz Hedayati
Bob Raymer
Frank Frievalt

This publication is available free of charge from:
<https://doi.org/10.6028/NIST.IR.8436>

**NIST Interagency Report
NIST IR 8436**

**Bounding the Structure Separation
Distance**

*A Modeling Study in Support of the Structure Separation
Experiments Project*

Kuldeep Prasad, Alexander
Maranghides, Eric Link, Shonali
Nazare, Matthew Hoehler, Matthew
Bundy, Rodney Bryant
*Fire Research Division
Engineering Laboratory*

Steve Hawks, Frank Bigelow
*Office of State Fire Marshall
California Department of Forestry and Fire
Protection*

William Mell, Anthony Bova,
Derek McNamara, Tom Milac
United States Forest Service

Daniel Gorham, Farz Hedayati
*Insurance Institute for Businesses and Home
Safety*

Bob Raymer
California Building Industry Association

Frank Frievalt
Mammoth Lakes Fire Protection District

This publication is available free of charge from:
<https://doi.org/10.6028/NIST.IR.8436>

October 2022



U.S. Department of Commerce
Gina M. Raimondo, Secretary

National Institute of Standards and Technology
Laurie E. Locascio, NIST Director and Under Secretary of Commerce for Standards and Technology

Certain commercial entities, equipment, or materials may be identified in this document in order to describe an experimental procedure or concept adequately. Such identification is not intended to imply recommendation or endorsement by the National Institute of Standards and Technology, nor is it intended to imply that the entities, materials, or equipment are necessarily the best available for the purpose.

NIST Technical Series Policies

[Copyright, Fair Use, and Licensing Statements](#)

[NIST Technical Series Publication Identifier Syntax](#)

Publication History

Approved by the NIST Editorial Review Board on 2022-09-12

How to Cite this NIST Technical Series Publication

Prasad K, Maranghides A, Link E, Nazare S, Hoehler M, Bundy M, Bryant R, Hawks S, Bigelow F, Mell W, Bova A, Milac T, Gorham D, Hedayati F, Raymer B, Frievald F (2022) Bounding the Structure Separation Distance: A Modeling Study in Support of the Structure Separation Experiments Project. (National Institute of Standards and Technology, Gaithersburg, MD), NIST Interagency Report (IR) NIST IR 8436.
<https://doi.org/10.6028/NIST.IR.8436>

NIST Author ORCID iDs

Shonali Nazare: 0000-0002-0407-5849

Matthew Hoehler: 0000-0002-6049-7560

Abstract

The primary objective of the Structure Separation Experiment project is to assess structure-to-structure fire spread for structures located in the wildland-urban interface (WUI). As part of this project, full scale fire experiments will be conducted in which various types of structures (sources of fire) will be used to generate typical radiative and convective heat exposures on target structures (residential dwellings). The spacing between the source and target structures will be varied to identify safe structure separation distance (SSD). Most experiments will be conducted with construction materials currently listed in State of California building codes and using code compliant structural assemblies. A limited number of experiments will be conducted with enhanced, ignition resistant, materials that may not currently be listed by the State of California.

The project is divided into three phases. Phase 1 will test sheds as fire sources, Phase 2 will test “in-law” buildings and Phase 3 will test single-family homes. Source terms from 1.39 m² to 24.8 m² (15 ft² to 267 ft²) will be tested in Phase 1. Phase 2 will examine exposures from a 40.87 m² (440 ft²) “in law” building and Phase 3 will characterize exposures from approximately 92.90 m² (1000 ft²) residences.

The goal of this report is to present a preliminary modeling approach for estimating an upper bound for the safe structure separation distance (SSD). This work is part of the larger modeling effort for the Structure Separation Experiments project and is intended to compliment the vast number of full-scale experiments that are being performed as part of this project.

Keywords

Heat Release Rate, Modeling, Structure Separation Distance; Wind; Wildland-Urban Interface.

Table of Contents

1. Modeling to Estimate Structure Separation Distance: Overview	1
2. Important Physical Processes and Modeling Challenges	1
2.1. Burner Placed in a Zero Ambient Wind Condition (Without a Target).....	2
2.2. Burner placed in an ambient condition (without a target).....	6
2.3. Comparison of fire plumes with Heskestad (1998) calculations.....	8
2.4. Effect of a real source (shed).....	9
2.5. Effect of target on the flow field.....	10
3. Estimating (bounding) Structure Separation Distance	11
4. Conclusions, Summary and Limitations	14

List of Tables

Table 1. Predicted ambient wind speeds using the Heskestad data, for various plume deflection angles.....	9
--	---

List of Figures

Fig. 1. Three-dimensional simulations of smoke and temperature contours above a burner. Simulation results are shown for heat release rates of 1, 2, 4, 8 and 16 MW (left to right).....	2
Fig. 2. Contours of vertical velocity in a plane perpendicular to the burner surface and passing through the center of the burner. Simulation results are shown for heat release rates of 1, 2, 4, 8 and 16 MW.	3
Fig. 3. Centerline plume vertical velocity (m/s) plotted in red, and temperature (°C) plotted in black, averaged over the last 10 seconds of the simulation. Results are plotted as a function of distance above the burner (m) for heat release rates of 1, 2, 4, 8 and 16 MW.	5
Fig. 4. Simulation of a 4 MW burner placed in an ambient wind of 2 m/s. Snapshot of the simulation results at the end of 100 s, show that the plume is leaning in the direction of the wind.	6
Fig. 5. Radiative heat flux and adiabatic surface temperature measured at different distances and heights above the burner surface. Red, Green and Blue curves are for gauges located at 3, 6 and 9 m from the downwind edge of the burner at a height of 3 m above the burner surface. Yellow, Cyan and Pink curves are for gauges located at 10, 20 and 30 ft from the burner at a height of 6 m above the burner surface.	7
Fig. 6. Heskestad (1998) correlation for flame deflection in ambient wind. Figure reproduced from Heskestad paper. Open symbols are from small-scale experiments by Welker & Sliopovich(1965) and solid circles are from large-scale LNG burns by Attalah & Raj (1974).	8
Fig. 7. Simulation of a 16 MW burner placed in an ambient wind of 4 m/s. Snapshot of the simulation results at the end of 100 s, show that the plume is leaning in the direction of the wind.	12
Fig. 8. Gas phase radiative heat flux measured at a height of 3 m above the burner surface with a heat release rate of 16 MW and an ambient wind speed of 4 m/s. The red curve shows the flux measured by a gauge pointing along the -ve x axis (towards the burner), while the blue curve shows the flux from a gauge pointing along the -ve y axis (downwards).	13
Fig. 9. Structure Separation Distance (SSD) in meters plotted as a function of the wind speed for various heat release rates from a one square meter burner. Results are shown for a target	

structure that is either facing upwind towards the burner or facing vertically downwards. The green region represents the current code provisions for structure separation distance.14

1. Modeling to Estimate Structure Separation Distance: Overview

The primary objective of the Structure Separation Experiment project Ref. [1] is to assess structure-to-structure fire spread for structures located in the wildland-urban interface (WUI). Full-scale fire experiments will be conducted in which various types of structures (sources of fire) will be used to generate typical radiative and convective heat exposures on target structures (residential dwellings). The spacing between the source and target structures will be varied to identify safe structure separation distance (SSD). Most experiments will be conducted with construction materials currently listed in State of California building codes and using code compliant structural assemblies. A limited number of experiments will be conducted with enhanced (ignition resistant) materials that may not currently be listed by the State of California Building Code Ref. [2].

Structure-to-structure fire spread occurs in WUI communities, when the source structure is located close to the target structure, which in turn results in radiative and convective heating of the target structure. The main goal of this component of the project is to develop a simple modeling approach for estimating an upper bound for safe structure to structure separation distance (SSD). Estimating the spacing between the source and target structure is critical for protecting communities from WUI fire spread, for retro-fitting of communities, and for developing building codes and standards.

As part of the modeling study, we will also attempt to validate the NIST Fire Dynamics Simulator (FDS) for specific outdoor experiments, with and without an ambient wind Ref. [3]. The modeling results that we present here can also be useful in designing structure separation experiments as well as test methods for codes and standards. Finally, the modeling study will aim to provide a methodology for scenarios where it is difficult to conduct experiments (sloping terrain etc.).

Modeling to estimate the safe separation distance between a real full scale fire source (burning shed, fence etc.) and a target (primary structure, walls, eaves, windows etc.) is a complex and challenging task. In this report we will systematically and gradually increase the complexity of the modeling simulations, starting from very simple configurations (burner placed in an ambient wind).

2. Important Physical Processes and Modeling Challenges

Estimating the safe separation distance between a real full scale fire source (shed or fence) and a target structure involves many complex physical and chemical processes. Any modeling approach that aims to estimate the safe separation distance between a source and a target should be able to resolve these important physical and chemical processes in an adequate manner. In this section, we describe these physical and chemical processes, starting from very simple configurations and gradually increase the level of complexity. For each scenario, we will first attempt to describe the processes and the capability of the state-of-the-art models to simulate these phenomena. Finally, we present a modeling scenario that is quite reliable (since it requires only one input parameter and can be validated with empirical relationships available in the literature) and can be used to provide an upper bound on the safe separation distance.

2.1. Burner Placed in a Zero Ambient Wind Condition (Without a Target)

The simplest scenario for estimating the safe separation distance is to consider a simple burner placed in a zero ambient wind scenario. Under this scenario, the fire source is replaced by a burner. We further assume that there is no target structure.

When there is no ambient wind, the hot combustion products from a burner rise vertically upwards due to their lower buoyancy. Modeling of a real burner under zero ambient wind involves turbulent entrainment of the surrounding air and mixing with the fuel gases. Modeling the turbulent entrainment and combustion (as an Arrhenius chemical process) requires a very fine computational mesh. In a real burner (such as the one used in NFRL), fuel gases come out of a system of tiny holes. Resolving the flow of the fuel gases places limitations on the mesh resolution, especially if the burner has a circular geometry that does not conform to the computational mesh.

A common technique used in computational modeling [3] is to dial in the heat release rate per unit area of the burner surface. The advantage of this methodology is that total heat released in the simulation is consistent with the measured heat released by the burner. This approach has the added benefit that the computational mesh does not have to be very fine to resolve the mixing processes and the combustion between the fuel and ambient air.

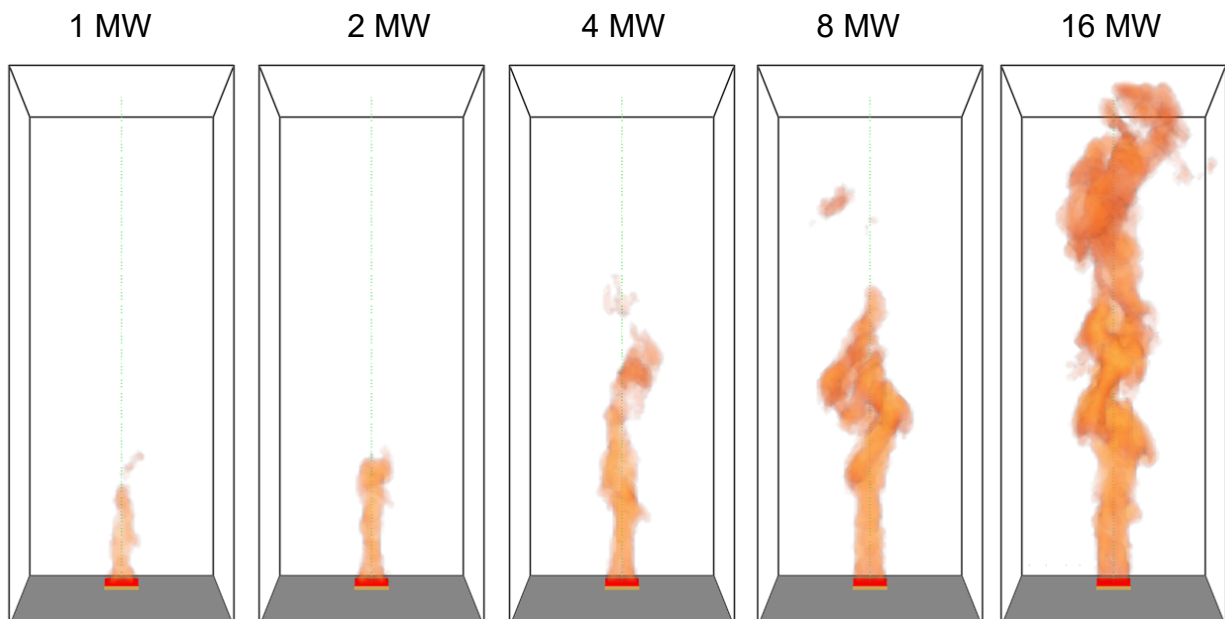


Fig. 1. Three-dimensional simulations of smoke and temperature contours above a burner. Simulation results are shown for heat release rates of 1, 2, 4, 8 and 16 MW (left to right).

A series of simulations were performed to simulate the dynamics above a simple burner in a zero ambient wind condition, using the NIST Fire Dynamics Simulator (FDS). The heat release rate per unit area of the burner surface was prescribed in these simulations. The heat release rate ranged between 1 MW and 16 MW. The goal of these simulations was to understand the predicted flame lengths as a function of the burner prescribed heat release rates and to compare these flame lengths with available data in the literature. A secondary goal of these simulations

was to understand the vertical gas velocities in the plume and heat flux levels at various distances from the burner.

The computational domain for the simulations was chosen as 6 m x 6 m x 15 m. A system of 12 meshes were used to grid the domain at a uniform spacing of 10 cm. A 1 m x 1 m square propane gas burner was located at a height of 0.5 m above the floor and a heat release rate per unit area (HRRPUA) was prescribed on the burner surface. Radiative properties for propane were used as follows (Radiative Fraction = 0.22, Soot Yield = 0.024, and CO Yield 0.005). Free slip wall boundary conditions were used on the floor, while the other walls of the computational domain were assumed to be open to allow for entrainment of the air into the plume.

Simulations were performed for a period of 30 seconds. The simulation period (30 s) is much larger than the transit time required for the gases to traverse the length of the computational domain. The temperature and velocities at several points along the centerline were monitored to ensure that the plume had achieved a quasi-steady state after 15 s of simulation.

Figure 1 shows visualization of the smoke and temperature contours Ref. [4] above a burner with heat release rates of 1, 2, 4, 8, and 16 MW. The heat release rate was a prescribed input value for the simulations and since the area of the burner was fixed, the fuel inlet velocity was changed to get the desired fuel flow rate. As the heat release rate increased the flame length increased as well. Figure 2 shows contours of vertical velocity in a plane perpendicular to the burner surface and passing through the center of the burner for the same heat release rates.

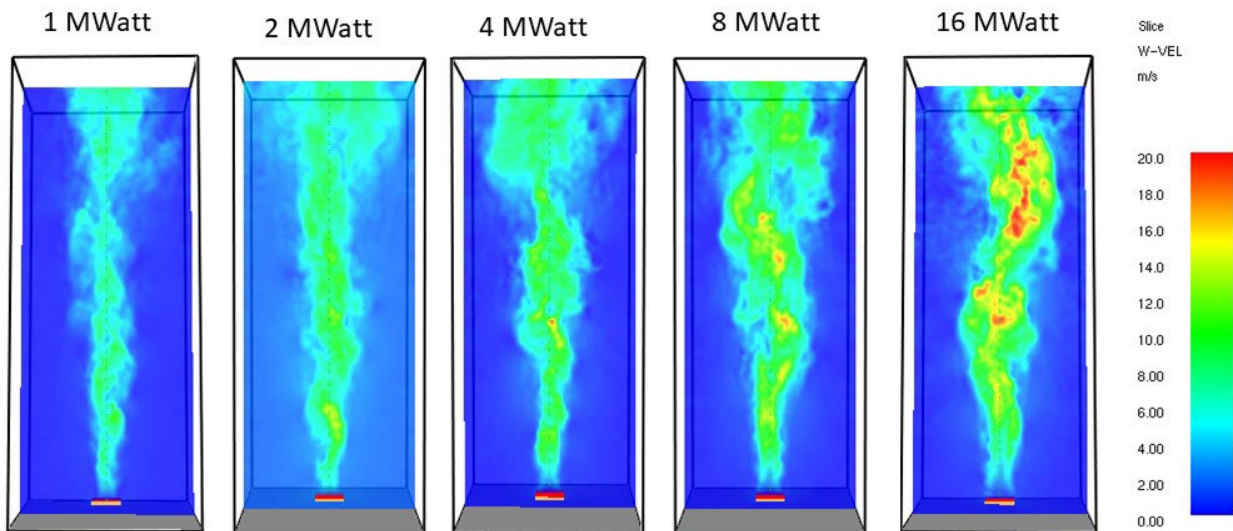


Fig. 2. Contours of vertical velocity in a plane perpendicular to the burner surface and passing through the center of the burner. Simulation results are shown for heat release rates of 1, 2, 4, 8 and 16 MW.

Center-line velocities and temperature over the entire length of the plume were computed by averaging the simulation results over the last ten seconds, as shown in Figure 3. Results show that the plume vertical velocity increases from very small values on the burner surface to approximately 8 m/s at a height of 3.5 m above the surface for the 1 MW case. The temperature also increases quickly, reaches a peak value, and then reduces due to entrainment of air into the plume. The temperature and vertical plume velocity are being discussed here since they play a

critical role in determining the plume lean in the presence of an ambient wind (discussed in the next section).

The maximum flame temperature does not change significantly as the heat release rate increases from 1 MW to 16 MW. However, the height above the burner surface where the peak temperature occurs as well as the extent of the high temperature region increases with heat release rate.

The maximum plume vertical velocity does seem to increase with heat release rate. As with the temperature profile, the height above the burner surface where the maximum velocity value is obtained as well as the extent of the region increases with heat release rate.

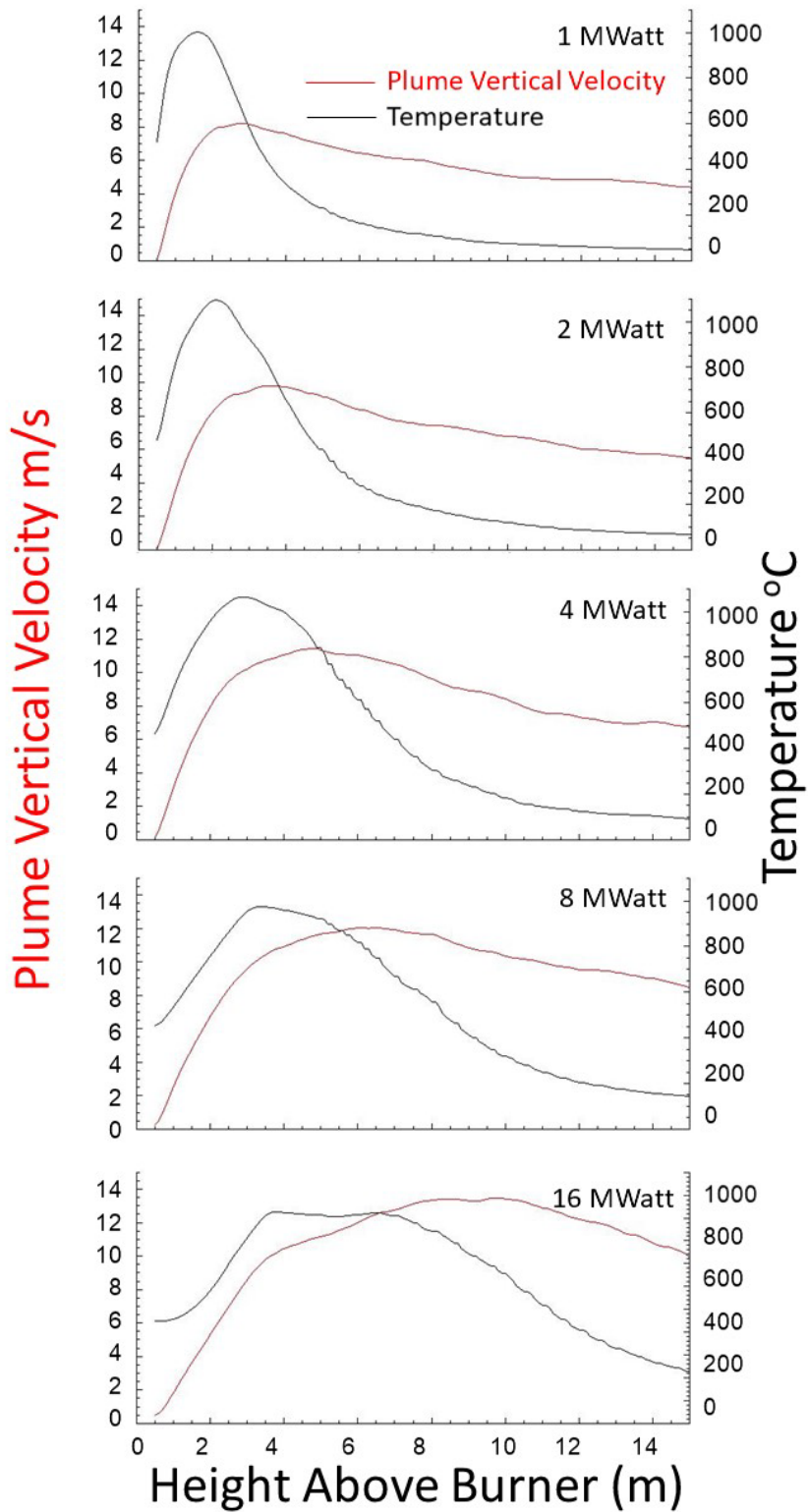


Fig. 3. Centerline plume vertical velocity (m/s) plotted in red, and temperature (°C) plotted in black, averaged over the last 10 seconds of the simulation. Results are plotted as a function of distance above the burner (m) for heat release rates of 1, 2, 4, 8 and 16 MW.

2.2. Burner placed in an ambient condition (without a target)

If the burner is placed in an ambient wind, then the buoyant plume of hot gases can bend in the direction of the ambient wind (flame tilt) and the flame can stretch and become diluted [5]-[12]. Both these effects are important since they affect the radiative and convective flux on a target structure placed downstream of the source.

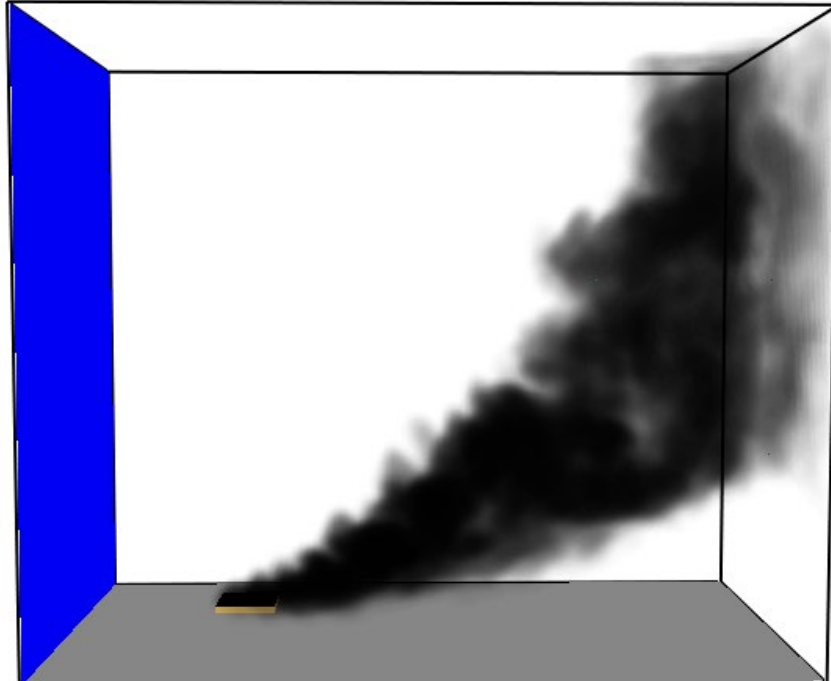


Fig. 4. Simulation of a 4 MW burner placed in an ambient wind of 2 m/s. Snapshot of the simulation results at the end of 100 s show that the plume is leaning in the direction of the wind.

FDS simulations were performed to visualize the plume lean in the presence of an ambient wind. The computational domain for the simulations was chosen as 21 m x 6 m x 10 m. A system of 28 meshes were used to grid the domain at a uniform spacing of 10 cm. A 1 m x 1 m square propane gas burner was located at a height of 0.5 m above the floor and a heat release rate per unit area (HRRPUA) was prescribed on the burner surface. The center of the burner had the following coordinates (3.0, 0.0, 0.5). Radiative properties for propane were used for the burner (Radiative Fraction = 0.22, Soot Yield = 0.024, and CO Yield 0.005). Free slip wall boundary conditions were used on the floor, a uniform wall of wind (plug flow) boundary condition was specified on the left wall, while the other walls of the computational domain were assumed to be open to allow for entrainment of the air into the plume.

Figure 4 shows typical smokeview visualization of a 4 MW burner placed in an ambient wind of 2 m/s. Simulation results clearly indicate that the plume bends and leans towards a potential target structure placed downwind of the source. Simulations were performed for heat release rates of 1, 2, 4, 8 and 16 MW and wind speeds ranging from 1 – 20 m/s.

For very small (low) ambient winds, the plume rose almost vertically upwards. As the ambient wind speed increases, the plume would lean into the wind as shown in Fig. 4. The flame tilt is usually defined as the angle the plume makes with the vertical Ref. [5]-[12]. As a result, the flame tilt angle is approximately 0 degrees for very low ambient wind, and it increases gradually as the ambient wind speed increases.

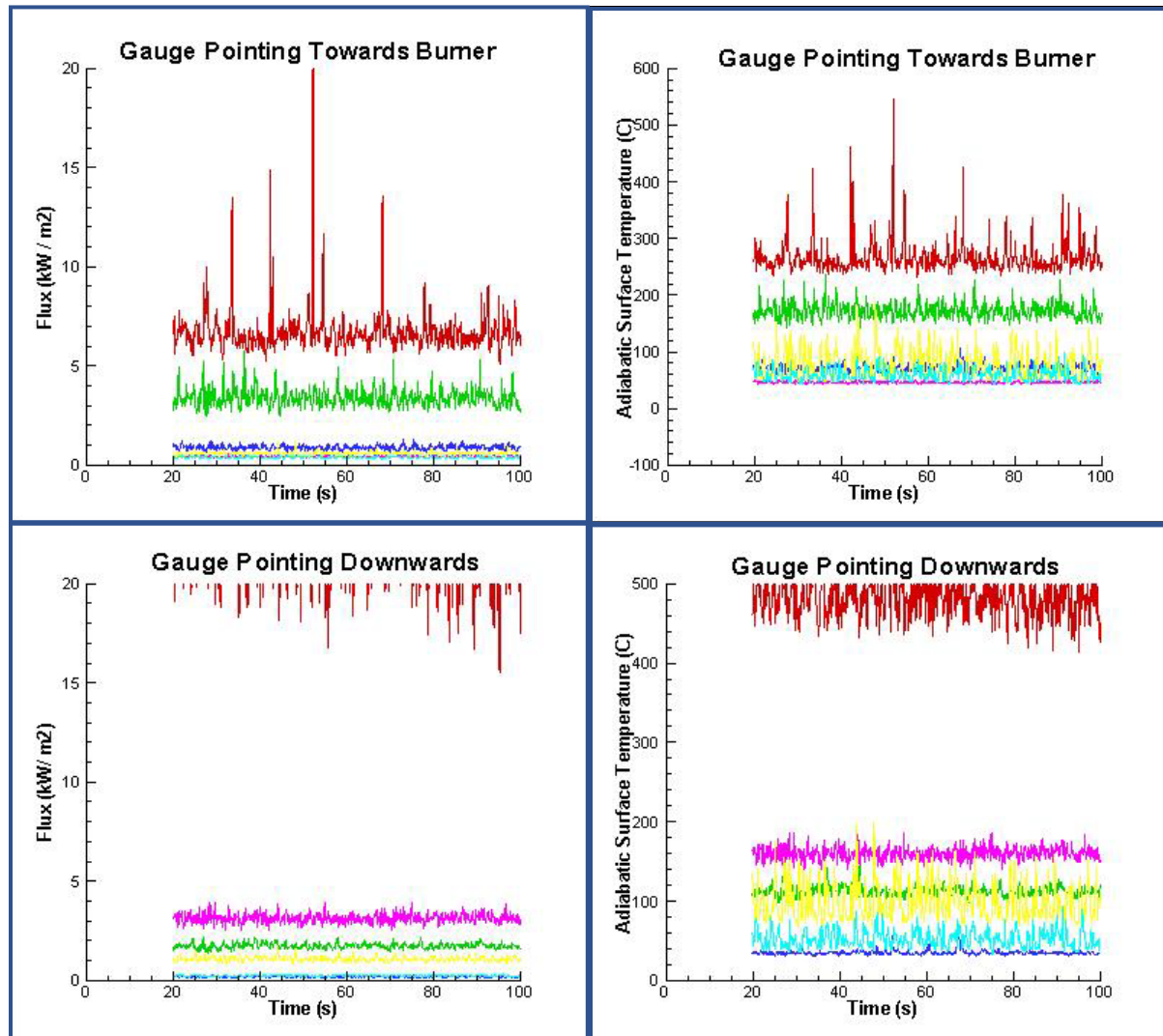


Fig. 5. Radiative heat flux and adiabatic surface temperature measured at different distances and heights above the burner surface. Red, Green and Blue curves are for gauges located at 3, 6 and 9 m from the downwind edge of the burner at a height of 3 m above the burner surface. Yellow, Cyan and Pink curves are for gauges located at 3, 6 and 9 m from the burner at a height of 6 m above the burner surface.

Figure 5 shows the radiative flux and adiabatic surface temperature for gauges pointing towards the burner or downwards. Results are shown for the last 80 seconds of the simulation, where steady state conditions have been achieved (as seen in the radiative flux plots). Red, green and blue curves are for gauges located at 3, 6 and 9 m from the downwind edge of the burner at a height of 3 m above the burner surface. Yellow, cyan and pink curves are for gauges located at 3,

6 and 9 m from the burner at a height of 6 m above the burner surface. The height of 3 m and 6 m roughly correspond to the height of the eaves for a 1 story or a 2 story building.

Results clearly indicate that the radiative flux varies with distance from the burner as well as height above the burner. Small variability in radiative flux measured at any gauge is due to the presence of vortices in the plume. Depending on the ambient wind conditions and heat release rate of the plume, the plume tilt can vary, which in turn can change the measured radiative flux. Higher radiative flux usually results in larger adiabatic surface temperatures as shown in Fig. 5. The adiabatic surface temperature is a measure of the maximum temperature that could be reached on the surface, assuming that there are no heat losses.

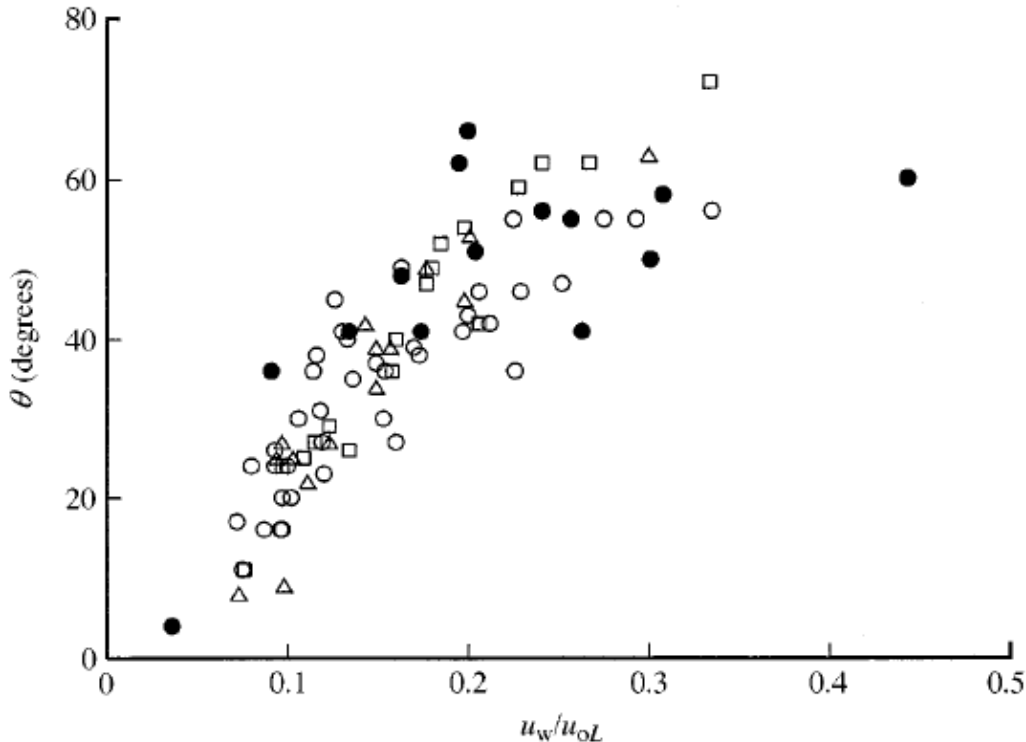


Fig. 6. Heskestad (1998) correlation for flame deflection in ambient wind. Figure reproduced from Heskestad paper. Open symbols are from small-scale experiments by Welker & Slipevich [6] and solid circles are from large-scale LNG burns by Attalah & Raj [7].

2.3. Comparison of fire plumes with Heskestad (1998) calculations

In this section, we present the approach that was used to compare / validate the plume deflection angles with Heskestad correlations. The overall goal for this section is to check if FDS simulations can adequately predict the plume deflection. It should be noted that if the flame deflections are predicted correctly, then it is more likely that the radiative flux will also be predicted correctly.

Figure 6 shows the Heskestad correlation for flame deflections in ambient wind. The plot shows the flame deflection angle plotted as a function of the ratio of wind speed (u_w) and plume velocity (u_{oL}).

For a given heat release rate per unit area, we first compute the plume velocity using the simulations described in section 2.1. The plume velocity profile for various heat release rates has been shown in Fig. 3. The maximum plume velocity is used for the purpose of this analysis as suggested in the paper by Heskestad et al. [12]. We now select an ambient wind speed and find the ratio of the maximum plume velocity to the ambient wind speed. Using Heskestad correlation plot (Fig. 6), we can now determine the flame deflection angle. We also ran an FDS simulations using the prescribed heat release rate and the selected ambient wind speed and estimate the flame deflection angle from the FDS simulations. The estimated flame deflection angle from the FDS simulations was compared with that obtained from the Heskestad correlations. Simulation results indicate that the plume deflection angle compared favorably with the Heskestad correlation, indicating that the simulations were able to predict the plume deflection (results of this analysis are summarized in Table 1).

Table 1. Predicted ambient wind speeds using the Heskestad data, for various plume deflection angles.

HRR (Mwatt)	Maximum plume speed u_{oL} (m/s) (20 s Average)	Predicted Ambient wind speeds u_w (m/s) for various plume deflections from vertical			
		20° (0.09)	40° (0.15)	60° (0.28)	80° (0.45)* <u>Extrapolated</u>
1	8.0	0.7	1.2	2.2	3.6
2	9.0	0.8	1.4	2.5	4.1
4	10.5	0.9	1.6	2.9	4.7
8	12	1.1	1.8	3.4	5.4
16	14	1.3	2.1	3.9	6.3

2.4. Effect of a real source (shed)

We have seen so far that CFD modeling can adequately and accurately capture the physics of a plume leaning into the ambient wind. Introducing a real source such as a burning wooden shed, or a fence can add new physical processes that can prove to be difficult to model.

Burning of a wood / steel shed that contains wood cribs is a complex process. As the wood cribs inside the shed are ignited, the fire initially spreads slowly through the cribs.

Modeling flame spread on a wooden crib involves many complex physical and chemical processes. Currently, there are no validation studies for flame spread over a single slab of wood in perfect laboratory conditions. Modeling of wood slabs stacked horizontally and vertically inside a small enclosure (where oxygen may be limited) is a complex process that is very challenging to model using CFD techniques.

At some point the wood cribs can ignite the wooden shed. This can result in the presence of two different peaks in the total heat release rate curve. The wooden cribs that have been burning for a while, can start collapsing and may lose their structural integrity. This can happen with the woodshed as well. Initially, we observe that the smoke usually flows out through the open doors. As the fires grow inside the shed, the glass windows of the shed may be compromised, and

smoke can pour out through the windows. This also can open additional pathways for the oxygen to enter the shed and support the intense combustion processes.

Numerically modeling the time when the glass windows get compromised or the cribs lose their structural integrity is a very difficult task for any CFD model. Modeling the changing geometry may be important in determining the heat release rate and oxygen that is required to support the combustion activities.

At some point during the burning, the roof of a wooden shed can collapse (fully or partially) and this can result in the fire plume shooting vertically upwards, instead of flowing through the open doors. Again, these are very complex events that are difficult to simulate using CFD models.

A real source also acts like an obstruction to the ambient flow field. It diverts the air around the source structure and produces a dead zone behind the source structure. This region, where the wind speeds are very small, may be an ideal location for smoldering combustion and ignition that can grow into larger fires. Again, these are very complex physical processes for which FDS has not yet been validated fully.

In summary, incorporating a real source in a simulation can result in several new physical processes that are very difficult to model using state of the art CFD techniques. In this report, we use a simple square burner with a steady heat release rate as the source. Our goal for this study is to estimate the structure separation distance for the worst-case scenario. For a realistic scenario (with a real shed), we anticipate that the structure separation distance will be smaller than our estimated structure separation distance using a burner.

2.5. Effect of target on the flow field

The presence of the target structure also affects the plume dynamics and imposes constraints on the computational method. The target structure blocks and diverts the air flow / plume. If the target walls are aligned with the computational mesh, they act like a bluff body that results in a dead zone before and after the target structure. This dead-zone region can also include a re-circulating zone that can be very conducive for firebrands to settle down, instead of being carried by the ambient wind. The low-speed region provides an ideal environment for ignition of the target material.

When the walls of the target structure are oriented an angle, they do not act as a bluff body, but only split or divert the plume around the target structure. However, from a computational point of view, this introduces new challenges. Since the walls are not aligned with the mesh, one can make use of a stair-step pattern to model the walls. This is not ideal, especially if the underlying grid resolution is coarse, which it usually is for the full-scale geometries that are under consideration.

Another option is to use the Immersed Boundary Method (IBM) that is currently under development in FDS to model the walls that are not aligned with the cartesian mesh. However, the IBM method currently does not handle heat transfer very accurately Ref. [3], and its use for target walls is not very helpful, since the primary purpose of the target walls is to understand the heating / ignition of the target structure. It has also been noticed that the IBM method requires much higher resolution, which again increases computation costs.

In any case, the roof of the target structure is usually not aligned with the underlying mesh. This leaves very few good options for modeling target structures that are not aligned with the computational mesh.

Overall, the presence of the source and / or the target structure can only slow the overall flow-field, due to the associated viscous effects, even though the flow may accelerate / de-accelerate locally. Neither structure can add energy to the ambient flow and as a result, the presence of these structures will only reduce the estimate of the safe separation distance.

3. Estimating (bounding) Structure Separation Distance

The presence of a burning source as well as a target structure can make the modeling tasks extremely difficult. We believe that the presence of source / target structure will end up reducing the structure separation distance.

The goal of this section is to estimate an upper bound for the safe separation distance. Based on the discussion seen in previous sections, CFD models can adequately predict the plume lean from a burner with a prescribed heat release rate and placed in a uniform ambient wind. We have demonstrated and validated that FDS can correctly predict the flame lean by comparing the simulation results with Heskestad's empirical correlations (Table 1). Since the flame lean is predicted correctly, it is believed that the radiative and convective flux from the plume to a target structure will also be predicted correctly.

In this section we describe the methodology that was used to estimate an upper bound for the structure separation distance. A series of simulations were performed to simulate the plume dynamics above a simple burner in uniform ambient wind condition, using the NIST Fire Dynamics Simulator (FDS). The goal of these simulations was to estimate and bound the structure separation distance for various burner heat release rate and wind speed scenarios.

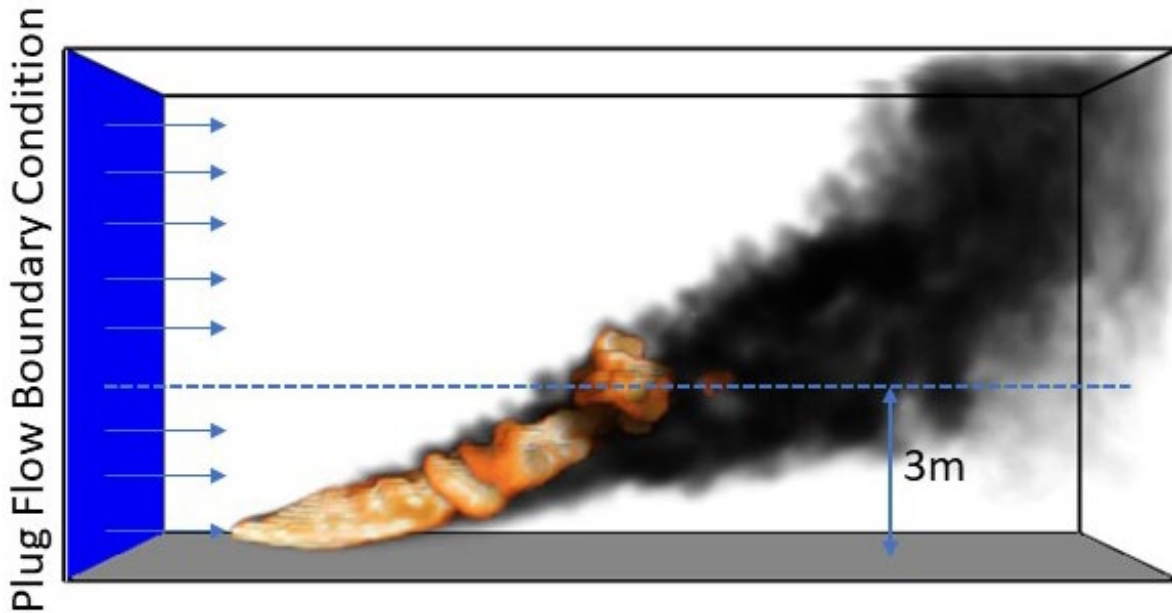


Fig. 7. Simulation of a 16 MW burner placed in an ambient wind of 4 m/s. Snapshot of the simulation results at the end of 100 s, show that the plume is leaning in the direction of the wind.

The computational domain for the simulations was chosen as 21 m x 6 m x 10 m shown in Fig. 7. A system of 28 meshes were used to grid the domain at a uniform spacing of 10 cm. A 1 m x 1 m square propane gas burner was located at a height of 0.5 m above the floor and a heat release rate per unit area (HRRPUA) was prescribed on the burner surface. The center of the burner had the following co-ordinates (3.0, 0.0, 0.5). Radiative properties for propane were used for the burner (Radiative Fraction = 0.22, Soot Yield = 0.024, and CO Yield 0.005). Grid resolution studies were performed by reducing the grid size to 5 cm, and it was found that the results / conclusions presented in this report were not affected significantly by reducing the grid size.

A uniform wind (plug flow boundary condition) was specified at the up-stream boundary. Simulations were performed with wind speeds ranging from 1-16 m/s. Free slip wall boundary conditions were used on the floor, while the other walls of the computational domain were assumed to be open to allow for entrainment of the air into the plume as well as for the flow of the hot gases out of the domain. Simulations were performed for a period of 20 seconds. Typical residence time of the gases is less than 10 seconds, even for the smallest ambient flow speeds under consideration.

Gas phase radiative flux gauges were placed at a height of 3 m above the burner surface as shown in Fig. 7. The height of 3 m was chosen because we are interested in single story structures, where the roofline is typically at a height of 10 ft. Two sets of measurements were made:

- a) Radiative flux measurement with a gauge pointing towards the burner (pointing along the -ve x direction), measuring the horizontal flux to a target structure such as the burner walls.

- b) Radiative flux pointing downwards (pointing along the -ve z direction), measuring the vertical flux to a target structure such as the eaves.

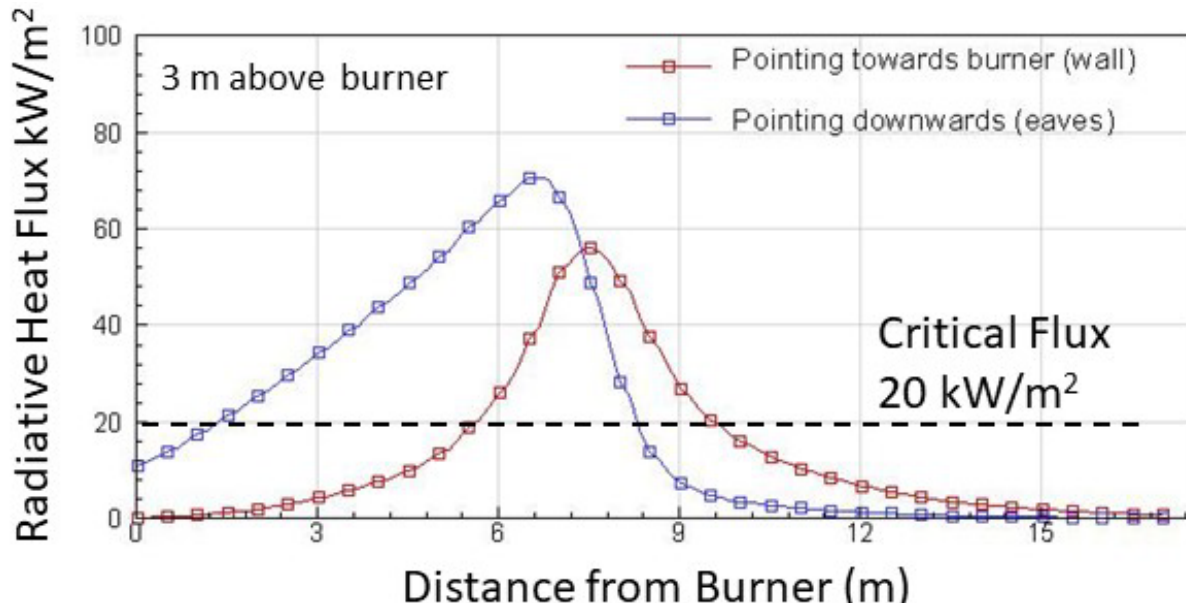


Fig. 8. Gas phase radiative heat flux measured at a height of 3 m above the burner surface with a heat release rate of 16 MW and an ambient wind speed of 4 m/s. The red curve shows the flux measured by a gauge pointing along the -ve x axis (towards the burner), while the blue curve shows the flux from a gauge pointing along the -ve y axis (downwards).

Figure 8 shows the radiative flux measured by a gauge pointing towards the burner (red) as well as by a gauge pointing downwards (blue). The heat release rate of the burner was 16 MW and the ambient wind speed was 4 m/s. Radiative flux is plotted at a height of 3 m above the burner surface.

The radiative flux gauge pointing downwards starts out at approximately 12 kW/m², and steadily rises to over 70 kW/m². During this portion, the plume is located below 3m (height of the gauge). The gauge pointing downwards reaches a peak value at a distance of 6.5 m from the burner. This is the point where the center of the plume (highest temperature) reaches the flux gauge. Beyond this point the plume is above the flux gauge, while the gauge is looking downwards. As a result, the measured radiative flux drops rapidly to small values.

The radiative flux gauge pointing towards the burner starts out at almost zero value and reaches a peak value of ~55 kW/m² at approximately 7 m from the burner. Beyond this, the flux values drop symmetrically to zero values. Peak values coincide with the point where the centerline of the plume is at the height of the gauge itself.

Figure 8 also marks out the critical flux horizontal line of 20 kW/m². In this report, we use this critical flux value as a threshold for ignition. This critical flux value has been derived from and is consistent with cone calorimeter experiment studies that indicate a minimum flux value for ignition of wood to be approximately 20 kW/m². Using the critical flux value and the radiative flux values in Fig. 8 we can predict the separation distance for a given heat release rate and wind speed. For It should be pointed out that 20 kW/m² is a rough approximation for ignition flux and

should be verified through full scale experiments. In this case, for an ambient wind speed of 4 m/s, the Structure Separation Distance (SSD) is 9.6 m for the wall and 8.3 m for the eaves.

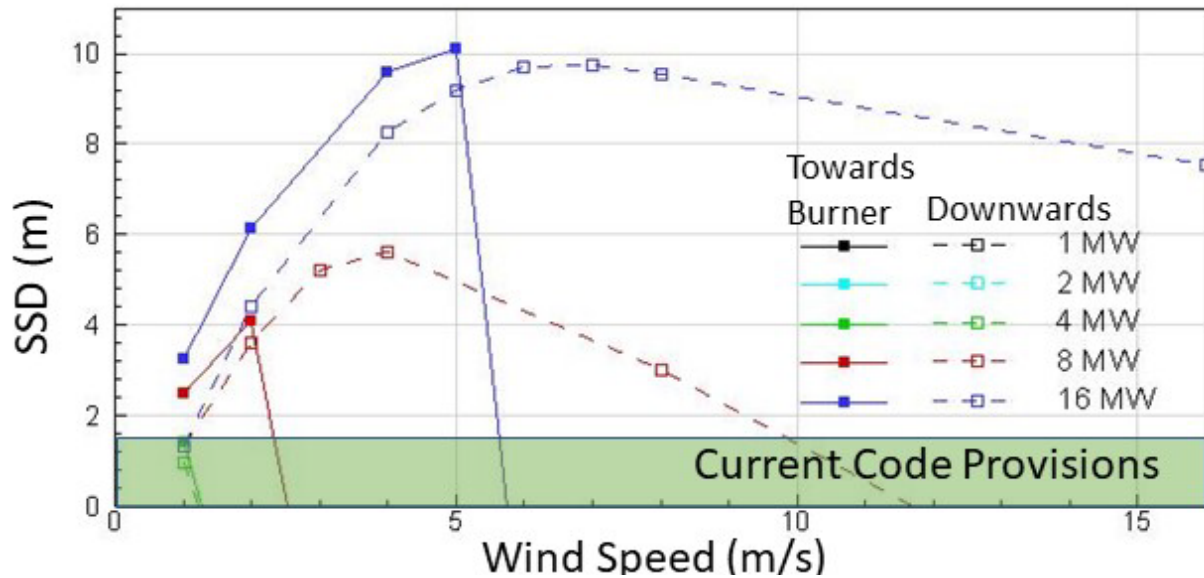


Fig. 9. Structure Separation Distance (SSD) in meters plotted as a function of the wind speed for various heat release rates from a one square meter burner. Results are shown for a target structure that is either facing upwind towards the burner or facing vertically downwards. The green region represents the current code provisions for structure separation distance.

Figure 9 shows the computed structure separation distance (m) plotted for various burner heat release rates and wind speeds. The SSD distance is shown in solid lines for gauge pointing towards burner and dashed lines for gauge pointing downwards. For a burner heat release rate of 16 kW, the SSD (computed from a gauge pointing towards burner) increases with wind speed, reaches a maximum value of approximately 10 m, at a wind speed of 5 m/s and then reduces quickly. The results for a gauge pointing downwards are similar, although the drop in SSD after the peak value is more gradual.

The computed SSD can be considered as the worst-case scenario or maximum SSD for the given heat release rate and wind speed conditions. The presence of a shed or a target structure will only slow the ambient flow-field through the creation of dead-zones, re-circulating zones, turbulence and viscous losses. As long as the heat release rate of the burner is the peak heat release rate of the source (shed), the computed safe separation distance using the method described in this report will represent an upper bound or worst-case limit.

4. Conclusions, Summary and Limitations

In this report, we have presented a simple, easy to use methodology to estimate an upper bound for the safe separation distance. Improvements to the analysis can include

- a) In this analysis we dial in the heat release rate and use the simulation results to predict the gas phase radiative flux. The radiative flux can be a function of the Radiative Fraction or Soot Yield (input parameters of an FDS simulation). A validation study for the predicted

flux from an FDS simulation over the entire range of heat release rate would be very helpful.

- b) The analysis presented in this report is based on the radiative flux to the structure. It is assumed that the convective flux is small. An improvement to the analysis would be to use both the convective and radiative flux for computing the safe separation distance.
- c) The role of slope can be incorporated in the FDS simulations by changing the direction of the gravity vector in the simulations that have been presented in this report.
- d) The heat release rate per unit area for the burner is an input parameter for the simulations. Ideally, this should be the maximum heat release rate from a full-scale calorimetry experiment performed under a hood. We do not have good experimental data for actual HRR during the burning of large sheds in the open.
- e) Although we don't expect major changes to the key results presented in this report, a systematic grid resolution study as well as the effect of changing the domain size should be considered.
- f) The burner size used in the simulations was set at 1 X 1 m. An exhaustive study should be conducted to understand the role of burner size on the results presented in this report.
- g) The methodology proposed in this report does not account for ignition due to embers. This is perhaps the biggest limitation of the current work.

References

- [1] A. Maranghides et. al, Structure Separation Experiments Phase 1 Preliminary Test Plan, NIST Technical Note 2161, <https://doi.org/10.6028/NIST.TN.2161>, May 2021
- [2] California Building Code-Chapter 7A-Materials and construction methods for exterior wildfire exposure. Available at <https://up.codes/viewer/california/ca-building-code-2016/chapter/7A/sfm-materials-and-construction-methods-for-exterior-wildfire-exposure#7A>
- [3] K. B. McGrattan, H.R. Baum, R. Rehm, A. Hamins, G. P. Forney, J. E. Floyd, S. Hostikka, K. Prasad, Fire Dynamics Simulator User's Guide. NISTIR 6783, U.S. Department of Commerce, National Institute of Standards and Technology, Gaithersburg, MD, 2002.
- [4] G. P. Forney, Smokeview - A tool for visualizing Fire Dynamics Simulation Data Volume 1: User's Guide, NIST Special Publication 1017-1, 2019.
- [5] G. Heskestad, Engineering relations for fire plumes, Fire Safety Journal, Volume 7, Issue 1, 1984, Pages 25-32.
- [6] Welker, J. R. & Sliepcevich, C. M. 1965 The effect of wind on flames. Technical Report No. 2, NBS Contract CST 1142 with University of Oklahoma.
- [7] Attalah, S. & Raj, P. K. 1974 Radiation from LNG fires. In Interim Report on Phase H Work. American Gas Association Project IS-3.1 LNG Safety Program.

- [8] F. Nmira et. al, Numerical study of wind effects on the characteristics of flames from non-propagating vegetation fires, *Fire Safety Journal*, 45 (2010) 129-141
- [9] R. M. Nelson, Re-analysis of wind and slope effects on flame characteristics of Mediterranean shrub fires, *International Journal of Wildland Fire* 2015, 24, 1001-1007
- [10] A. Tohidi & N. B. Kaye, Highly buoyant bent-over plumes in a boundary layer, *Atmospheric Environment*, 131 (2016) 97-114
- [11] E. Eftekharian et. al, Investigation of fire-driven cross-wind velocity enhancement, *International Journal of Thermal Sciences* 141 (2019) 84-95
- [12] G. Heskestad, Dynamics of the fire plume, *Phil. Trans. R. Soc. Lond. A* (1998) 356, 2815-2833.